PNAS RESEARCH ARTICLE | NEUROSCIENCE
PSYCHOLOGICAL AND COGNITIVE SCIENCES

Innate face-selectivity in the brain of young domestic chicks

Dmitry Kobylkov[a], Orsola Rosa-Salva[a], Mirko Zanon[a], and Giorgio Vallortigara[a,1]

Edited by Robert Seyfarth, University of Pennsylvania, Philadelphia, PA; received May 25, 2024; accepted August 19, 2024

Shortly after birth, both naïve animals and newborn babies exhibit a spontaneous attraction to faces and face-like stimuli. While neurons selectively responding to faces have been found in the inferotemporal cortex of adult primates, face-selective domains in the brains of young monkeys seem to develop only later in life after exposure to faces. This has fueled a debate on the role of experience in the development of face-detector mechanisms, since face preferences are well documented in naïve animals, such as domestic chicks reared without exposure to faces. Here, we demonstrate that neurons in a higher-order processing brain area of one-week-old face-naïve domestic chicks selectively respond to a face-like configuration. Our single-cell recordings show that these neurons do not respond to alternative configurations or isolated facial features. Moreover, the population activity of face-selective neurons accurately encoded the face-like stimulus as a unique category. Thus, our findings show that face selectivity is present in the brains of very young animals without preexisting experience.

face perception | NCL | electrophysiology | innate | birds

Significance

Multiple behavioral studies have suggested that face selectivity might be an inborn feature of the brain. Both newborn human babies and newly hatched domestic chicks that have never seen faces before show spontaneous attraction toward face-like stimuli composed of three dark features representing eyes and a mouth/beak. However, the neural mechanism of this innate predisposition has remained unknown. By recording single-cell neural responses to face-like stimuli in young face-naïve domestic chicks we revealed a population of neurons selectively responding to a canonical face-like configuration, compared to alternative configurations or isolated facial features. This result shows that face-responsive neurons in the brain of young chicks emerge before any experience, supported by evolutionarily predisposed innate mechanisms.

Face perception is a fundamental set of cognitive skills (1). In fact, our visual system is so primed to faces that we can recognize face-like patterns even in inanimate objects like clouds or the Moon, a phenomenon known as pareidolia. This is true not only for humans: For other animals too, faces and facial features are highly salient, playing an important role in social interactions [mammals (2), birds (3–5), fish (6), and even insects (7)]. Birds have been shown to use facial features for individual recognition [budgerigars (8); pigeons (9)] and sexual selection (3). Apart from the social context, a face might also signal a presence of a predator (10).

Over the last four decades, significant progress has been made in understanding the neural mechanism of face perception. Neurons specifically responding to monkey and human faces have been found in the inferotemporal cortex (IT) of adult primates (11, 12) and the fusiform gyrus of humans (for a review see ref. 13). These neurons show a strong selectivity to faces compared to other visual or auditory stimuli (but see ref. 14). A crucial question, however, is whether this selectivity is only the result of experience or whether is it supported by evolutionarily predisposed innate mechanisms.

Several lines of evidence support the idea that face detection mechanisms might be present from birth. Multiple studies have shown that behavioral responses to faces emerge very early in development. Newborn babies are attracted by a schematic upright face-like pattern with two eyes symmetrically placed above the mouth (15, 16). This behavioral bias has been observed in human fetuses in utero, where human fetuses reacted more to the upright face than to the inverted stimulus (17). In a precocial species, domestic chicks, a similar preference for face-like stimuli has been found soon after hatching before they had ever seen a face (4). At the neural level too, face-selective neural responses have been recorded in the electroencephalogram (EEG) of newborn babies (18) and the hemodynamic response (fMRI) of young infants (19).

However, in contrast, fMRI evidence from monkeys suggests that face-selective domains (inferotemporal areas that are specialized for face processing) develop through extensive early-life experience with faces. Face domains were absent/underdeveloped in monkeys younger than 3 mo (20) or raised without exposure to faces (21). These results have fueled a debate on the origins of face-selective neural responses, which is far from being resolved.

For instance, the hypothesis of an acquired mechanism of face detection does not account for the evidence of behavioral biases toward faces. Spontaneous face-preferences emerge before the development of the face-selective cortical domains (21) and do not require preexposure to faces (4, 5). On the other hand, the face-naïve monkeys tested by Arcaro et al. (21) were deprived of visual experience with faces for several months. Such long-lasting deprivation from biologically relevant sensory stimuli is known to alter cortical development (22). The underdevelopment of the face domains in face-naïve monkeys could simply reflect this prolonged deprivation, rather than prove the absence of an evolutionary predisposed, innate neural mechanism tuned to faces. Thus, exposure to faces

Author affiliations: [a]Centre for Mind/Brain Science, University of Trento, Rovereto 38068, Italy

Author contributions: D.K., O.R.-S, and G.V. designed research; D.K. performed research; D.K. and M.Z. analyzed data; and D.K., O.R.-S., M.Z., and G.V. wrote the paper.

The authors declare no competing interest.

This article is a PNAS Direct Submission.

[1]To whom correspondence may be addressed. Email: giorgio.vallortigara@unitn.it.

This article contains supporting information online at https://www.pnas.org/lookup/suppl/doi:10.1073/pnas.2410404121/-/DCSupplemental.

Published September 24, 2024.

during sensitive developmental periods might be necessary for the maintenance rather than for the development of face selectivity in the brain. In addition, the fMRI itself is probably not sensitive enough to detect single-cell face-selective responses in very young animals, which may precede the formation of face domains. For example, in infant monkeys, Rodman et al. (23) did find face neurons, albeit with firing rates substantially lower than in adults. Thus, in the current discussion on the developmental origin of face detection, one of the main stumbling points is that so far none of the studies could detect single-cell neural responses to faces in newborn face-naive animals (24).

By recording single-cell neural activity in the nidopallium caudolaterale (NCL) of newly hatched chicks (Figs. 1*A* and 2*A*), we were able to study innate face-selectivity, while avoiding long deprivation phases. The NCL is a higher-order processing area of the bird telencephalon (25) involved in a wide array of cognitive functions, including object categorization (26). As a center for multimodal integration, the NCL receives information from both the avian lemnothalamic and collothalamic pathways. The latter provides the major source of visual input to the nidopallium via the superior colliculus homologue (27), which has been hypothesized to support automatic orientation to faces (28) and terminates in the entopallium, which corresponds to mammalian extrastriate cortices (29). This pathway is crucial for object detection and categorization (30) similar to the ventral stream (or "what pathway") in mammals (31). Moreover, in primates, face-processing regions such as the occipital face area (OFA), the fusiform face area (FFA), and the anterior temporal lobe face area (ATL-FA) are also located in the ventral visual stream (32). Therefore, although there are no direct homologues of these mammalian cortical regions in the avian pallium, the NCL as an associative area integrating most of the visual input to the avian telencephalon is a promising candidate to search for face-selective responses.

While most of the studies that investigated neural responses to faces employed realistic face images, the studies that revealed early face-preference in human newborns (15, 16) and newly hatched chicks (4) have typically used highly simplified schematic face-like stimuli (Fig. 1*D*). This approach, that represents the accepted

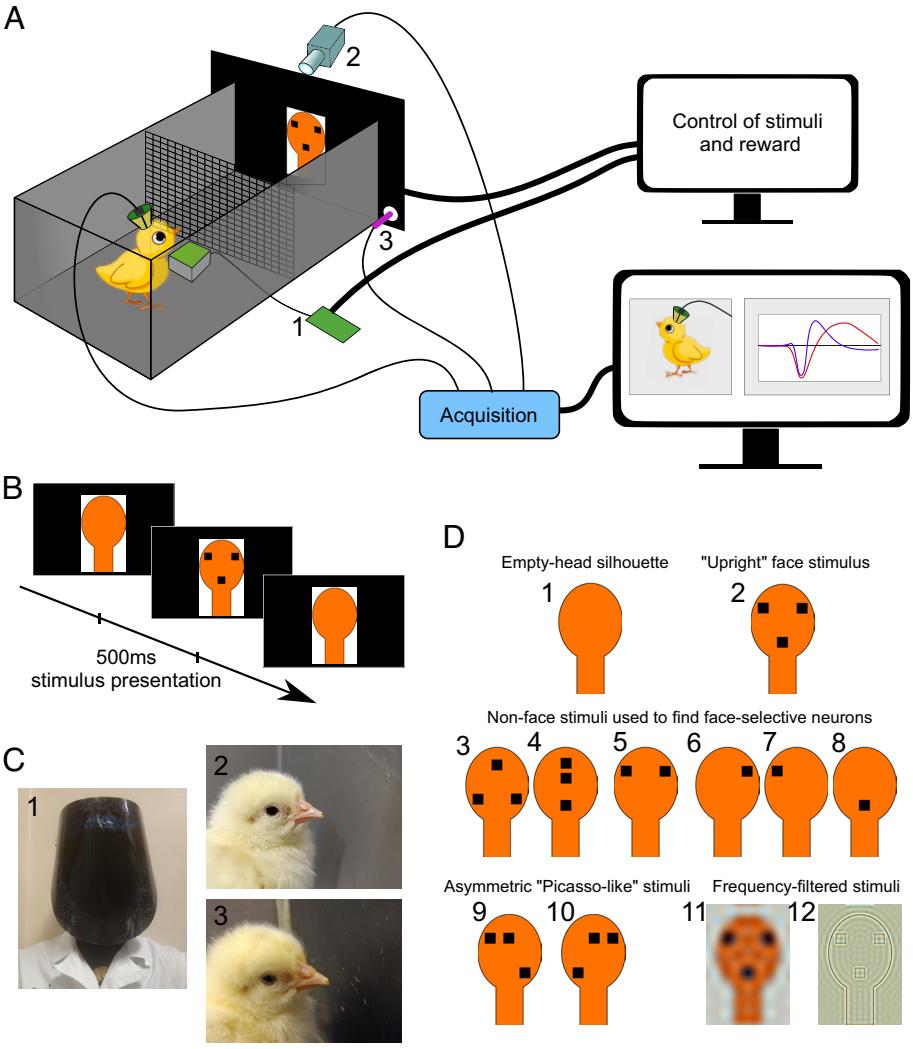

Fig. 1. Experimental setup and stimuli. (*A*) The schematic of the experimental setup. Chicks were observing stimuli on a computer monitor. To enhance the motivation of birds to pay attention to the screen, random trials were occasionally rewarded [(1) feeder controlled by Arduino]. The trials were video recorded (2) and the timing of stimuli was controlled by a photodiode (3). (*B*) Face-like configurations were presented randomly for 500 ms on an empty-head silhouette. (*C*) The chicks did not have any previous experience with faces: the experimenter was wearing a black-painted mask (1), housing cages (2), and the experimental cage (3) were made of nonreflective materials. (*D*) Experimental stimuli. (1) An empty head silhouette used for habituation and as a background image during stimuli presentation. Thus, in each trial only the configuration of dots inside this head region (2 to 10) or the frequency components of the stimulus (11, 12) was changing. We defined a face detector based on its significantly stronger response to the "upright" face-like configuration (2) than to other geometrical configurations with three dots ["inverted" (3) and "linear" (4)] or to single facial features: "eyes" (5), "left eye" (6), "right eye" (7), "beak" (8). Furthermore, we tested the response of putative face neurons to asymmetrical "Picasso-like" stimuli with eyes shifted from the medial sagittal line to the right ["picassoR" (9)] or to the left ["picassoL" (10)]. In addition, we tested how face neurons respond to face-like stimuli dominated by low-frequency (11) or high-frequency (12) components.

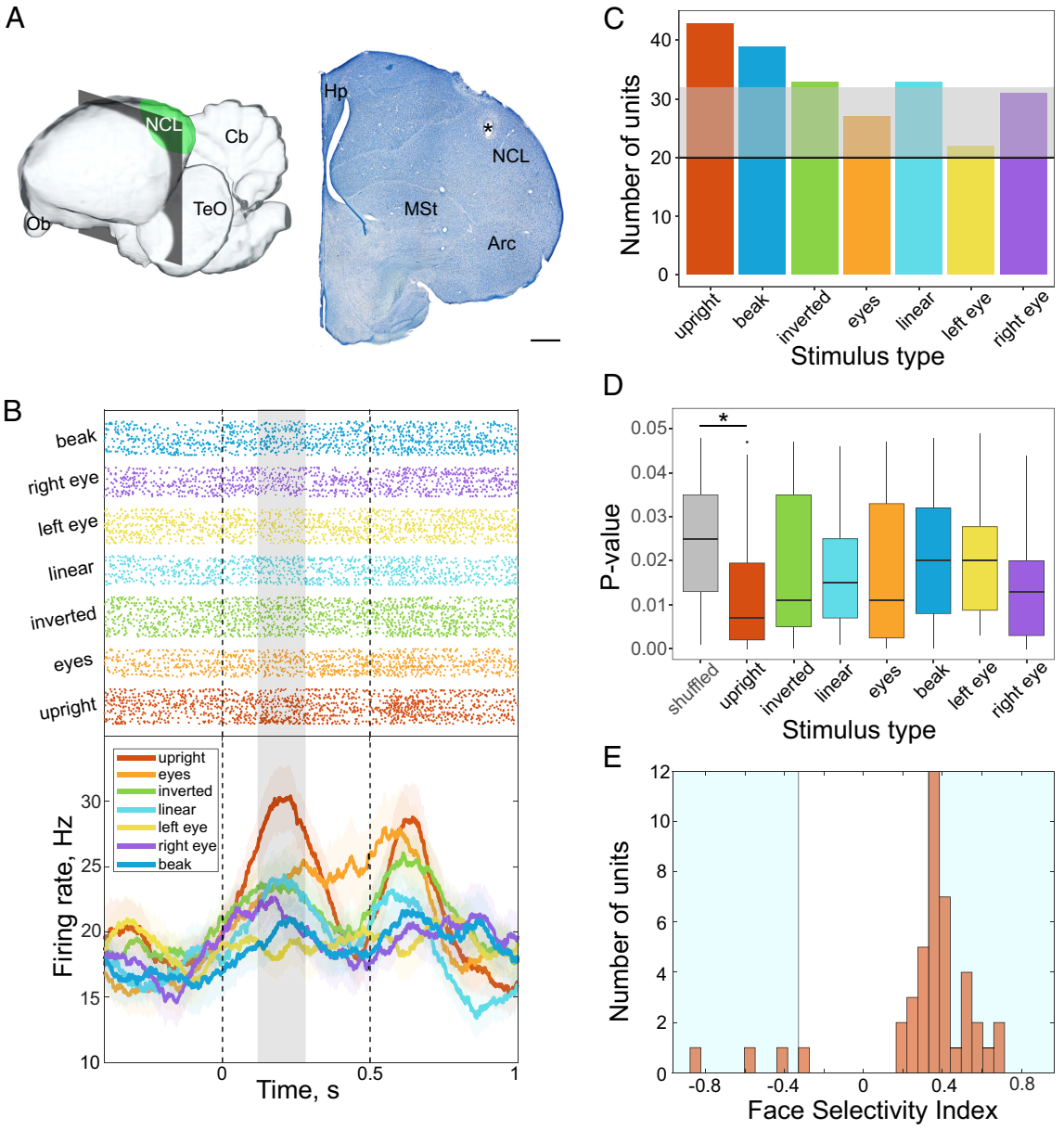

Fig. 2. Face-selective neurons in the NCL of young domestic chicks. (*A*) Recording site localization within the caudolateral nidopallium (NCL) of young domestic chicks. On the *Left*, the approximate location of the NCL in the avian brain is highlighted in green, while the gray-shaded plane shows the rostro-caudal position of the brain section presented in the other half of the figure. On the *Right*, Giemsa staining of a coronal brain section shows the electrical lesion's location at the recording site (marked with an asterisk). (Scale bar, 1 mm.) Abbreviations: Arc, arcopallium; Cb, cerebellum; Hp, hippocampus; MSt, medial striatum; NCL, caudolateral nidopallium; Ob, olfactory bulb; and TeO, optic tectum. (*B*) Example of a unit that responded significantly stronger to the upright stimulus. The raster plot in the upper part depicts trial-by-trial neural responses grouped by stimuli types (shown in different colors). Each line in the raster plot represents a single trial, with neural spikes marked by dots. The peristimulus time-histogram (PSTH) in the lower part represents the average neural responses to stimuli smoothed by the Gaussian kernel (100 ms sigma). The shadowing around each curve in the PSTHs marks the SEM neural response. The gray shadow indicates the face-selective time window. (*C*) Number of units that showed selective responses to different configurations of face-like stimuli. The chance level and the corresponding 95% CI are indicated, respectively, by the solid black line and the gray shadowing (chance level is set at 20 units, which corresponds to the proportion of stimulus-selective units emerging as false positive from the analysis of shuffled trials). (*D*) Distribution of the *P*-values yielded for the selective windows of actual stimulus-selective units and of false-positive units resulting from shuffled trials (in gray). The actual face-selective neurons had lower *P*-values than false-positives [ANOVA $P = 0.016$ (DF = 7, F = 2.51); Tukey–Kramer test: $^*P = 0.03$]. In contrast, the distribution of *p*-values for the other types of stimulus-selective units was not significantly different from that of the false positive units. (*E*) Distribution of the face-selectivity index (FSI), which quantifies the selectivity of each face-responsive cell. A FSI ≥ 0.33 or ≤ −0.33 (shown with light-blue shadows) corresponds to a 2:1 ratio in responsiveness between face vs. nonface responses and is considered a strong selectivity (positive values indicate excitatory units, while negative ones correspond to inhibitory units).

standard in the developmental literature (15–18), showed that the innate response to faces is triggered mainly by the geometrical configuration of facial features, which may be considered as a "supernormal stimulus" sensu ethology (33). This characteristic arrangement of facial features is particularly important for the face-detection mechanism, which serves as broad filter and rapidly drives attention to stimuli that resemble a face in their overall configuration (28, 34, 35). Therefore, to investigate face-selective responses in the NCL of chicks we employed a schematic face-like stimulus, featuring two dark spots symmetrically positioned above the mouth/beak, forming an upside-down triangle within the head silhouette (Fig. 1 *D*, 2). This configuration triggers robust behavioral preferences and is recognized as "face-like" from early development through adulthood (36). This simplified stimulus also controls for the influence of high-level visual features and allows assessment of the impact of individual facial features and their

configurations. With this approach, here we demonstrate that neural face selectivity can emerge without specific prior experience by recording electrophysiological responses to face-like stimuli in young chicks that had never been exposed to faces.

Results

To identify face-selective neurons in young chicks, we compared single-cell electrophysiological responses to several configurations of face-like stimuli. Putative face-selective neurons responded more strongly to the upright stimulus with the normal configuration of facial features compared to either an incomplete face (eyes, beak, left eye, right eye; Fig. 1 *D*, 5–8) or a different configuration of facial features (inverted, linear; see Fig. 1 *D*, 3 and 4). We further characterized the response of identified face-selective neurons to asymmetric stimuli (Picasso-like faces), which violate the symmetrical configuration of the face template (Fig. 1 *D*, 9 and 10). Based on existing behavioral evidence, we expected innate face responses to be reduced for these asymmetric stimuli in chicks (4) (but see ref. 37). Furthermore, we tested whether face-selective neurons would be sensitive to the spatial frequency content of the face-like stimulus, as innate face detectors have been hypothesized to selectively respond to the low-spatial frequency content of the image (28). Consequently, we expected face-selective responses to be reduced for high-pass filtered images ("HF") compared to low-pass ("LF") filtered ones (Fig. 1 *D*, 11 and 12).

8% of NCL Neurons Selectively Respond to the Upright Face Configuration. We recorded neural activity from 540 neurons in the NCL of young face-naïve domestic chicks (Fig. 2*A*). To identify stimulus-selective neural responses we performed a sliding-window ANOVA (one-way ANOVA). The raw neural response in every trial was first smoothed using a Gaussian kernel with 100 ms sigma and then divided into 10-ms intervals. These intervals were compared with one-way ANOVA using the stimulus type as a factor (seven stimuli types: upright, inverted, linear, eyes, left eye, right eye, beak) and Tukey–Kramer post hoc tests to select only those intervals, where the response to a particular configuration was significantly different from all other stimuli. The longest continuous period (at least 100 ms) in which the neural response to one of the stimuli was significantly different from all other stimuli (permutation test, $P < 0.05$) was defined as a stimulus-selective window (see *Materials and Methods* for details). In this way, we identified 8% of all recorded units (N = 43) as face-selective (or face-responsive) neurons. The proportion of face-selective units did not differ significantly between individuals ranging from 6 to 10% (proportion test: $P = 0.84$), including the animal with the recording from the left hemisphere. Face-selective units exhibited significantly stronger responses to the upright face-like stimulus, than to single facial features (eyes, beak, left eye, right eye) or to alternative arrangements of these features (inverted, linear; see Fig. 2*B* and Movie S1 showing exemplary face-selective neural responses). We also did not observe any gradual decrease in the response of face-selective neurons to different nonface stimuli (*SI Appendix*, Fig. S1).

The number of face-selective neurons was significantly higher than what expected by chance (proportion test: $P < 0.001$, $\chi^2 = 12.09$, Fig. 2*C*). The number of stimulus-selective units expected by chance was estimated by conducting the same sliding-window ANOVA, but on shuffled trials (each recorded trial is randomly assigned to a stimulus type). Over 1,000 iterations of this shuffled trials analysis, 3.7% of units randomly appear to be selective for one of the stimulus types (false-positive units). While the majority of the recorded stimulus-selective neurons preferred the upright face configuration, we also observed selective responses to other tested stimuli, especially the beak, as visible in Fig. 2*C*. Selective responses to the beak (7.2%, N = 39) occurred significantly more often than expected by the chance level (proportion test: $P = 0.003$, $\chi^2 = 8.54$). In contrast, the number of selective responses to facial features in other configurations (inverted and linear, 6% N = 33 each) was barely above the chance level (proportion test: $P = 0.04$, $\chi^2 = 4.16$).

We further compared the distribution of the *P*-values that the permutation test yielded for face-selective neurons, compared to that of false-positive units obtained from shuffled trials. While selective windows in real and false-positive units were defined based on the same criterion, the *P*-values of real face-selective neurons were significantly lower than those of false-positive neurons [ANOVA $P = 0.016$ ($DF = 7$, $F = 2.51$); post hoc Tukey–Kramer test: $P = 0.03$; Fig. 2*D*]. However, this was not the case for real neurons selective for other stimulus types.

Consistent with our selection criteria, during the face-selective response window, face-responsive neurons showed a strong preference for the upright face configuration compared to other stimuli. This was quantified by their FSI [FSI = 0.41 ± 0.14, Mean ± SD (38)]. The majority of the face-selective units (74%, N = 32) had an absolute FSI of 0.33 or higher (Fig. 2*E*), which means that their response to the upright face was at least two times stronger, in one or the other direction, than the averaged response to other nonface stimuli. Most face-selective units exhibited an excitatory response to the upright face stimulus, which is associated to a positive FSI (*Materials and Methods*). Only 9% (N = 4) of face-responsive neurons showed negative FSI, being selectively inhibited by the face stimulus.

Both excitatory and inhibitory face-responsive units were sensitive to the symmetry of the face stimulus, even though their responses were modulated in opposite directions [LME $P < 0.001$ ($numDF = 5$, $F = 26.29$) for the interaction factor "stimulus type" * "FSI," Fig. 3). Excitatory units (i.e., units with a positive FSI that increase their firing rate in response to the upright stimulus), showed a significantly reduced excitation (lower response) to the Picasso-like images [post hoc Tukey test: $P < 0.001$ for upright vs. picassoL ($z = 9.27$) and upright vs. picassoR ($z = 9.56$)]. Conversely, units with a negative FSI show significantly less inhibition (higher response) to the Picasso-like stimuli than to the face stimulus [post hoc Tukey test: $P = 0.014$ ($z = -3.13$) for upright vs. picassoL and $P = 0.046$ ($z = -2.73$) for upright vs. picassoR].

We additionally compared the neural responses of the face-selective cells to the images with the low- and high-frequency components. For inhibitory units, the response strength was significantly different between LF and HF stimuli [LME, $P = 0.02$ ($numDF = 3$, $F = 3.3$) for the interaction factor stimulus type * FSI, Fig. 4]. Units with a negative FSI showed significantly more inhibition in response to the LF than to HF stimulus [post hoc: $P = 0.032$ ($z = -2.6$)]. However, contrary to our expectations, there was no significant difference between these stimuli in the response strength of FSI positive units [post hoc: $P = 0.24$ ($z = 1.75$)].

Population Analysis. The face-selective window of face neurons was evenly distributed throughout the trial duration. For about one third of the units, the longest face-selective response window started even after the stimulus offset (as shown in the heatmap in Fig. 5). To evaluate the amount of information about the face-like stimuli contained in the entire population response throughout the trial, we calculated the percentage of variance explained (PEV) by the factor stimulus type. We found two significant windows, during which stimulus-specific information content affected the

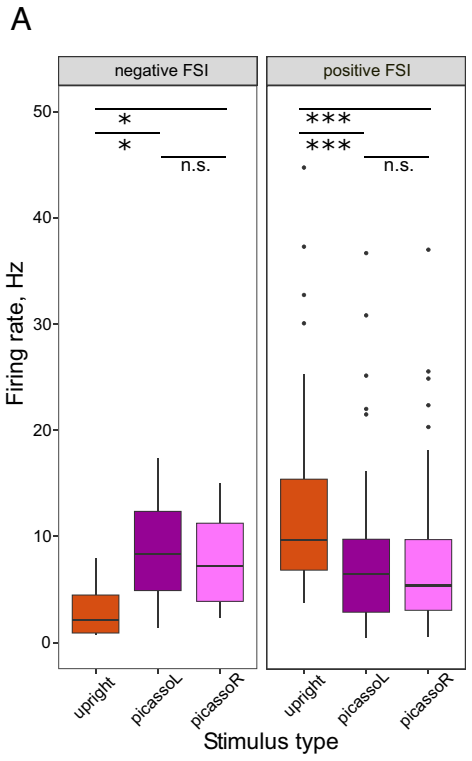

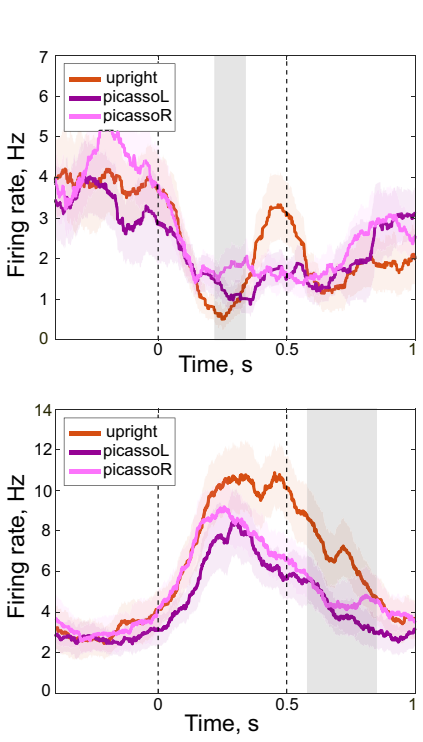

Fig. 3. The face-selective units showed sensitivity to the symmetry of the face stimulus. (*A*) The average firing rate within the face-selective window was significantly different between the upright symmetric face and Picasso-like stimuli with eyes shifted either to the left (picassoL) or to the right (picassoR). This effect acted in opposite directions for units with a negative and a positive FSI. Face-selective cells with a negative FSI ($N = 4$) showed reduced inhibition, while cells with a positive FSI ($N = 39$) showed reduced excitation to Picasso-like stimuli. Significance levels are based on the post hoc Tukey test of the linear mixed effect model: $^*P < 0.05$, $^{***}P < 0.001$, n.s., not significant. (*B*) PSTHs of two exemplary neurons with a negative and a positive FSI (upper and lower plot, respectively).

population response (a first peak between 130 ms and 380 ms after the stimulus onset and a second one between 430 ms and 630 ms, Fig. 5). This shows that the stimulus-specific information was retained by the population response even after the offset of the stimulus.

Decoding Analyses. To estimate whether the population activity can support an accurate categorization of face-like stimuli, we trained support vector machines (SVMs) on the neural responses of face-selective units to all stimuli. This included also the Picasso-like, the HF, and the LF images, the responses to which had not been used for the initial selection of face-selective units. We then tested the categorization performance of the SVMs on activity elicited by each stimulus type (with trials not presented at training).

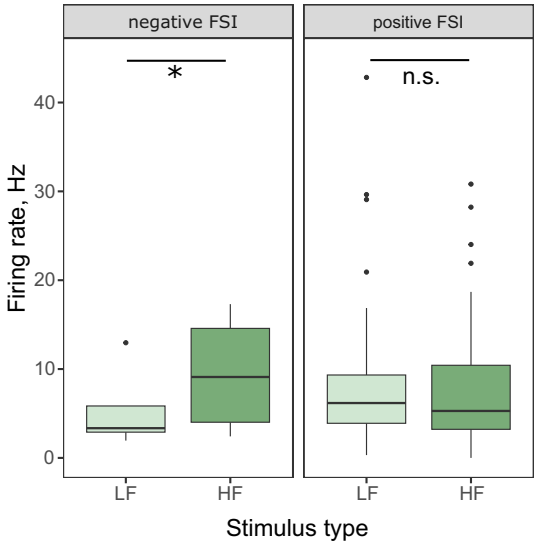

Fig. 4. Responses of the face-selective neurons to stimuli with the LF and HF components. The average firing rate within the face-selective window was significantly different between the LF and the HF only in units with the negative FSI ($N = 4$). Significance levels are based on the post hoc analysis of the linear mixed effect model: $^*P < 0.05$, n.s., not significant.

The SVMs trained on the face-selective response windows were able to successfully categorize the upright face with high accuracy (42%, proportion test: $P < 0.001$ ($\chi^2 = 581.09$), compared to the chance probability of 9%, Fig. 6*A*). The only stimuli that were mistakenly categorized as faces were asymmetric Picasso-like images [15%, $P < 0.001$, both for picassoL ($\chi^2 = 35.05$) and picassoR ($\chi^2 = 32.03$)]. Additionally, the same model was able to categorize HF and LF stimuli, which seemed to form a distinct category. Inverted and Picasso-like stimuli were also coded as distinct categories, meaning that the number of correct estimations for these categories exceeded the number of false assignments. Similar high decoding accuracy was observed in the SVMs trained separately on the units with the positive and the negative FSI (*SI Appendix*, Fig. S2*A*). The SVM trained on the average neural response of all recorded neurons was also able to uniquely decode the upright face configuration with the accuracy higher than the chance level [24%, proportion test: $P < 0.001$ ($\chi^2 = 80.57$), *SI Appendix*, Fig. S2*B*]. Notably, the SVM trained on all but face-selective units did not differentiate between the upright and the inverted configuration (*SI Appendix*, Fig. S2*B*).

To estimate how the accuracy of decoding changes over the time of the stimulus presentation, we applied Gaussian kernel smoothing (100 ms sigma) and trained SVMs on the consecutive 10 ms time bins for the whole duration of the trial. Interestingly, the accuracy of face-decoding was significantly above chance level starting already at 30 ms after the stimulus onset (Fig. 6*B*). This result, however, might be affected by the width of the Gaussian kernel (100 ms). Moreover, the accuracy remained significantly above chance during the whole trial, even after the offset of the stimulus.

SVMs trained on all stimulus types showed high decoding accuracy for upright face vs. other stimuli. Hence, we performed an additional generalization test by training SVMs to perform a binary

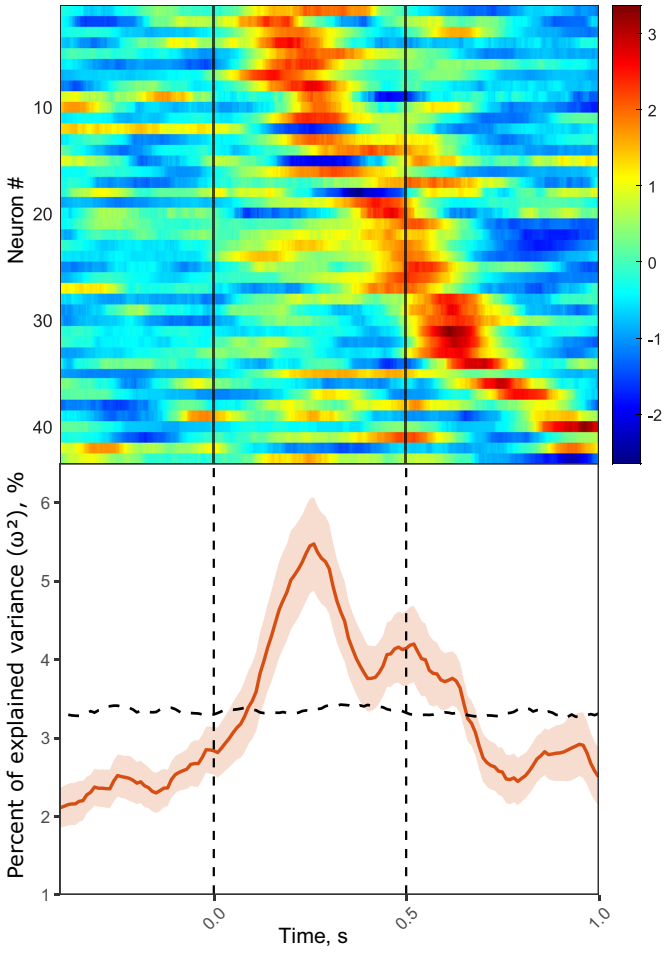

Fig. 5. Population analysis of face-selective neurons. The heatmap in the upper part shows the neural response of all face-selective neurons ($N = 43$): each line represents the neural activity of a single neuron. The raw neural activity was first smoothed with the Gaussian kernel (100 ms sigma), then averaged over all trials in which the upright face stimulus was presented, and finally z-scored. The color map ranges from deep blue to dark red, indicating low and high firing rate, respectively. The lower part of the figure shows the PEV (ω^2) by the factor stimulus type during the whole period of the trial (*Materials and Methods*). The horizontal dashed line marks the 95th percentile of the ω^2 obtained from shuffled data (corresponding to $P < 0.05$). Vertical lines delineate the onset and the offset of the stimulus.

face vs. nonface classification on all but one of the stimulus types (Fig. 6*C*). Subsequently, we tested the performance of the SVMs on the stimulus type not included into the training, to see whether these novel stimuli would be spontaneously classified as faces or nonfaces. We consecutively performed eight separate generalization tests on the following stimuli: eyes, inverted, linear, three-dots-stimuli (inverted and linear together), one-dot-stimuli (left eye, right eye, and beak together), Picasso-like stimuli (picassoL and picassoR together), HF, and LF. All tested stimuli were classified with high accuracy as nonfaces (eyes: 93%; inverted: 83%; linear: 95%; three-dots-stimuli: 89%; one-dot-stimuli: 96%; Picasso-like stimuli: 76%; HF: 89%; LF: 75%). However, it is interesting to note that Picasso-like and LF stimuli were classified as faces in ca. 25% of all cases, which is significantly higher than the proportion of false assignments (8%) during the test of the classifier (proportion test: $P < 0.001$, Picasso-like stimuli: $\chi^2 = 173.92$; LF: $\chi^2 = 194.5$).

Discussion

Single-cell responses to faces have not been previously described in newborn face-naïve animals. Here, we show that in one-week-old domestic chicks never exposed to faces, ca. 8% of all recorded neurons in the NCL selectively respond to a schematic face stimulus. The observed number of face-selective units was twice higher than what expected by chance. Moreover, as demonstrated by the analyses of the population response (PEV) and the decoder performance (SVM), these neurons constitute a neural population that encodes face-like stimuli as a separate category. The proportion of face-selective cells we found in the NCL of young chicks is comparable to what has been previously described in the temporal cortex of sheep [7% (39)] and in the superior temporal sulcus of monkeys [10% (12)]. At the same time, it is much lower than in specialized face-selective cortical patches of humans [54% (40)] and monkeys [75% of all recorded neurons (38)]. However, it is important to note that the face-selective cortical patches in primates were first identified with fMRI and only then targeted for single-cell recordings. One could thus speculate that areas with a higher density of face-selective neurons could be found in chicks too, if a similar approach were applied to identify recording locations. Moreover, face-selective neurons in monkeys and humans are usually defined based on their differential response to faces compared to objects/body parts (40, 41). In our case, all tested stimuli are considerably more similar to each other, which results in a stricter criterion for face selectivity. This is however also a partial limitation of our study, compared to the primate literature, since we did not test the responses of face-selective neurons to less controlled, but more naturalistic stimuli. Future studies should thus capitalize on our findings to further probe the generalizability of these neural responses to a wider range of stimuli and their role in inborn face preferences.

The majority of recorded face-selective neurons (74%) had a FSI of ≥0.33, i.e., their response to the upright face-like stimulus was at least twice as strong as to other configurations. At the same time, on average the FSI of face-selective neurons in the NCL of chicks was lower than what has been previously described for face neurons in primates (38). However, we believe that direct comparisons with studies in monkeys might be misleading for several reasons. First of all, in primates, neurons with high FSI have been found in highly selective cortical face patches predefined by fMRI, while we have recorded from the NCL, which is a large and widely unexplored brain area. The second important point is that compared to studies in monkeys, we have recorded from very young face-naïve animals. Hence, the response properties and the tuning of these neurons can change over time as it has been already shown for monkeys (23). The last, but not the least critical aspect refers to the very definition of the face-selectivity index. The magnitude of the FSI highly depends on the types of stimuli used in the experiment and in the analysis. In most of the studies on face perception in monkeys, a wide variety of nonface objects is used as stimuli (20, 21, 38, 42). These loosely defined nonface stimuli differ substantially from faces in their appearance and, hence, elicit generally a much weaker response. In this case, averaging of all responses to nonface stimuli increases the FSI. In our study, all visual stimuli are highly controlled, being very similar in terms of low-level visual features. Therefore, the difference in the neural response between the face- and the nonface configurations is less pronounced.

While the idea of innate face responses in the brain has been debated for a long time, the experimental evidence in support of this theory remained rather scarce (reviewed by ref. 43). Face-specific neural responses have been detected in the EEG of newborn babies already during the first days after birth (18). Still, even at this age in human babies, it is extremely difficult if not impossible to exclude the influence of exposure to faces. On the other hand, studies on face-deprived monkeys (20, 21) might be prone to artifacts related to possible side effects of long-lasting face deprivation.

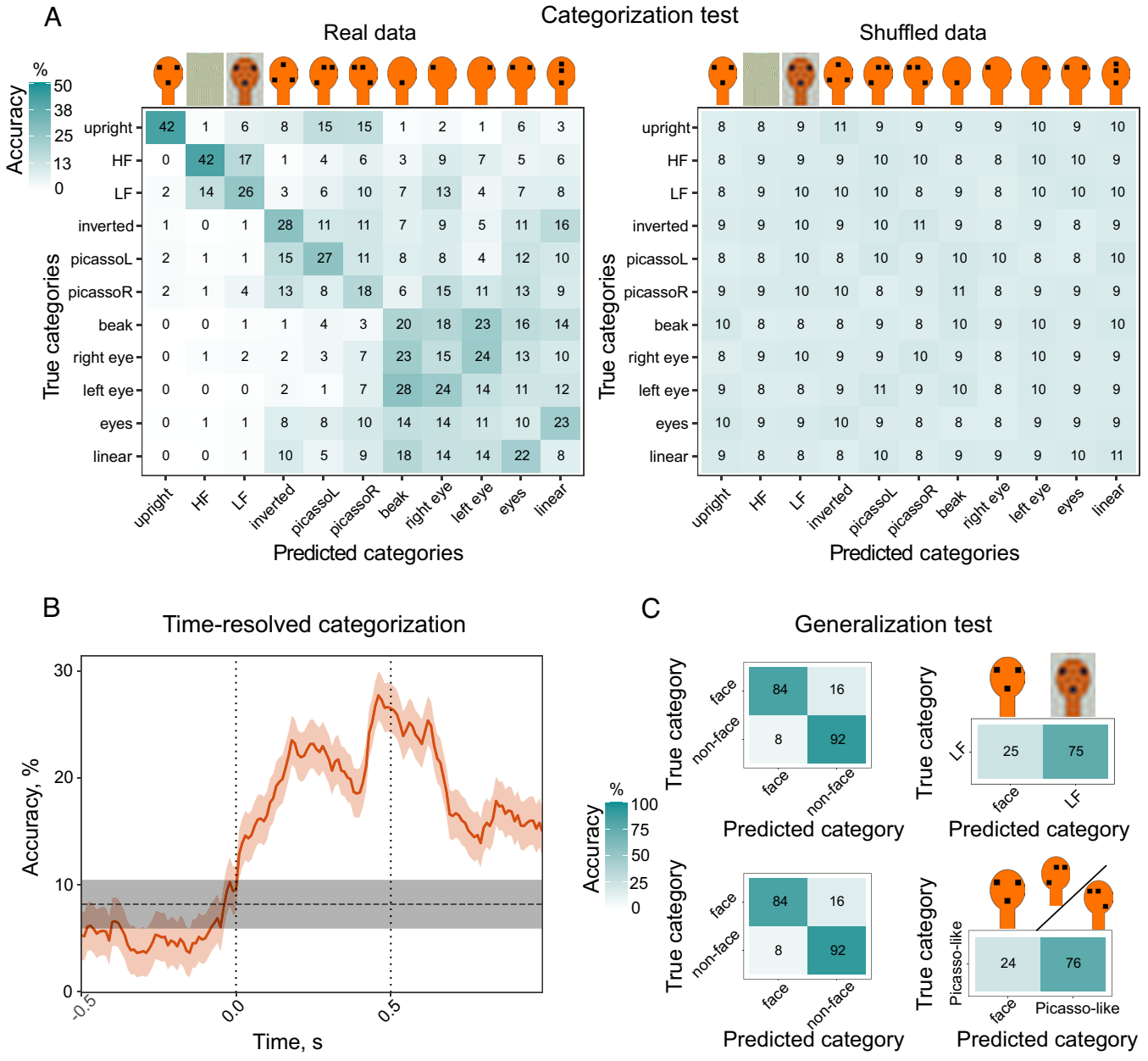

Fig. 6. Decoding analyses based on supervised training of SVMs. (*A*) A multiclass classifier (SVM) was trained on the trial-by-trial average firing rate within face-selective response windows. The confusion matrix on the *Left* shows the decoding accuracy of the classifier (in %). When the classifier was trained on shuffled data, its accuracy dropped to chance level (confusion matrix on the *Right*). (*B*) Time course of the decoding accuracy for the upright face-stimulus (orange line with shading: mean ± 95% CI). First, every trial was smoothed with the Gaussian kernel (100 ms sigma) and then the classifier was trained on the firing rate of consecutive 10 ms time bins. The classifier accuracy increased significantly above the chance level already 30 ms after the stimulus onset. The chance level (horizontal black line with shading) was calculated based on the classifier accuracy during the prestimulus 500 ms interval (*Materials and Methods*). The vertical dotted lines delineate the onset and the offset of the stimulus. (*C*) Generalization tests showing the performance of a binary classifier trained on all-but-one stimulus types. First, the classifier was trained to categorize stimuli into "face" and "nonface" classes based on the average firing rate within the face-selective window (*Upper* and *Lower Left* confusion matrix). Then, the classifier was asked to categorize the new stimulus type. The two confusion matrixes on the right illustrate the generalization performance for the LF stimulus (*Upper Right*) and the Picasso-like stimuli (*Lower Right* matrix).

By using precocial domestic chicks, we were able to minimize the face-deprivation period to a few days only and record neural activity in very young face-naïve animals. While chicks in our experiments were devoid of any experience with faces, it is virtually impossible to exclude all symmetrical visual stimuli from the environment (like corners of the cage or the black face-mask). Nevertheless, such an unspecific visual input could not explain our results. Most of the nonface control stimuli used in our experiments were symmetrical (eyes, inverted, linear, beak, HF, LF); however, there was no similarity between neural responses to these configurations and the upright face. On the contrary, the generalization analysis revealed similarities between the neural response of face-selective neurons to asymmetrical Picasso-like stimuli and to symmetrical upright faces (Fig. 6*A*). Hence, the observed face-selective neural responses correspond well with the spontaneous behavioral bias toward faces known in newly hatched chicks (4) and provide strong evidence that face selectivity in chicks is an inborn feature of the brain.

Contrary to the hypothesis of innate face-selective mechanisms, Arcaro and Livingstone (44) suggested an alternative explanation: early-life selectivity for faces could be attributed to an innate hierarchical proto-organization of the visual system. This innate

hierarchical map in monkeys would show selective responses only to low-level features like shape and spatial frequency. This organization might serve as a scaffold for further development of category-selective responses. This hypothesis, however, does not seem to explain our results. Our face-selective neurons showed significantly stronger responses to the upright face compared to the inverted and the linear configurations. Importantly, the upright face stimulus is virtually identical to the inverted and the linear ones in terms of spatial frequency and luminosity (*SI Appendix*, Fig. S3). Therefore, the selectivity of the neural response can originate solely from the specific face-like geometrical configuration. The functional role of the face-selective neurons in chicks has yet to be elucidated. This innate and potentially evolutionary conserved mechanism might be not directly involved in the recognition of individual conspecifics. Instead, it might reflect, directly or indirectly, the action of mechanisms for spontaneous detection of face-like patterns. These mechanisms likely serve to drive animals' attention to social stimuli, e.g., to facilitate imprinting in newborn animals. Even though the neural bases of innate face detectors are unknown, they have been hypothesized to reflect the action of subcortical regions, such as the superior colliculus and the pulvinar (28). NCL is unlikely to represent an early station for the rapid detection of face-like stimuli. However, it receives particularly abundant visual input from the avian collothalamic visual pathway, whose first stations are in the avian superior colliculus and pulvinar homologues (27). In line with that, many face-selective neurons responded to the face even after the stimulus offset. This was also reflected in the PEV and in the time-resolved SVM analyses, the latter showing high decoding accuracy for the upright face during the whole trial period. This delayed response suggests that at least some of the face-selective neurons in the NCL could be not sensory, but might be rather involved in further processing of faces and some executive functions associated with this biologically important stimulus. This would be in line with NCL's role in cognitive functions such as selective attention (45) and decision-making (46).

Notably, all previous attempts to find face cells in the avian brain have yielded underwhelming results (47–49). However, all previous studies in adult birds have used naturalistic images of faces. These birds/human faces are visually complex, with many local features, making it difficult to control relevant properties of the stimuli such as spatial frequency and luminosity. At the same time, even naturalistic face images still lack many aspects that might be important for birds' visual system: These are static images, presented on a flat screen, with colors that are unnatural to birds' vision. Since we do not know the relative importance of all these features for birds, they might perceive such "naturalistic" images as rather unnatural and confusing.

Contrary to realistic face images, the schematic face-like pattern employed in our study served as a supernormal stimulus, eliciting a strong selective response in the innate face-selective mechanisms (Fig. 1 *D*, 2). The face-selective neurons were sensitive not only to the particular number of visual elements (two eyes and a beak), but also to the specific geometric configuration and orientation of these elements. Their response to the geometrically identical, but inverted face was significantly reduced compared to the upright face stimulus with eyes placed above the beak. Similarly, in newborn human babies, inversion of the face stimulus also resulted in a weaker EEG response (18). The face inversion effect observed at the neural level underlies a well-known behavioral phenomenon: Inverted faces were shown to attract less attention in human babies (16) and in young chicks (4).

The difference in the neural response between upright and inverted faces cannot be explained by an attentional bias toward top-heavy stimuli, where more visual elements are concentrated in the upper part of the image (37, 50). In behavioral experiments, newly hatched chicks spontaneously prefer the normal-face configuration over the equally top-heavy linear stimulus (4). Likewise, in our study, neurons selective for the upright face configuration responded significantly less to the linear top-heavy stimulus. This confirms that the neurons we describe in the NCL of chicks are selective to the distinct face-like configuration, rather than to single visual elements or their arrangement per se.

Apart from the upright triangular configuration, the vertical symmetry of facial features is one of the main properties that might facilitate face detection. Face symmetry has been utilized to enhance algorithms for automatic face detection in silico (51). The face-selective neurons that we recorded in the brains of chicks also relied on face symmetry. These neurons had weaker responses to Picasso-like stimuli with eyes shifted to the side of the medial sagittal line. Accordingly, in behavioral experiments with face-naïve chicks, no preferences were found between Picasso-like and control stimuli (4). Interestingly, the analysis of the SVM classifier performance revealed a certain degree of similarity between Picasso-like and symmetric upright stimuli at the level of neural population response. The spontaneous categorization of Picasso-like stimuli as something in between a face and a nonface object has also been reported in humans. In newborn babies, the EEG response to asymmetric stimuli was closer to the normal upright face than to the inverted configuration (18). In human adults, fMRI revealed slightly different responses to Picasso's paintings with realistic and asymmetric faces (52).

Several studies have suggested that low- to mid-spatial-frequency components play a pivotal role in fast face detection (53, 54) (reviewed by ref. 55). In line with that, in our recordings, LF stimuli had a relatively high probability (25%) of being treated as faces by a classifier trained to categorize faces vs. nonfaces. Hence, there are similarities in the response of the neural population to normal and low-frequency filtered faces. Furthermore, units with a negative FSI (inhibited by upright faces), reduced their response to the LF compared to the HF stimuli. Units exhibiting a positive FSI, however, did not show significant differences between the neural responses to LF and HF stimuli. The relatively small difference between the responses to LF and HF stimuli might be explained by the reduced contrast they present compared to other stimuli due to filtering and subsequent luminance adjustment. Decreased contrast might have affected the perception of the frequency-filtered stimuli. This is indirectly supported by the analysis of the classifier performance, which shows a high level of similarity between LF and HF stimuli. Hence, the frequency-filtered stimuli, which differ in their contrast from the rest of the stimuli, could have triggered a specific neural response.

It is important to stress that the relative role of various spatial frequency components in face detection remains largely unexplored, particularly at the single-cell level. Rolls et al. (56) observed that face neurons in the superior temporal sulcus of monkeys respond to both low-pass and high-pass filtered faces, although with reduced amplitude. Results from EEG (57) and MEG (54) also suggest that fast and accurate face detection depends on the combination of both high and low-spatial frequency information. Moreover, according to fMRI data, the low-spatial-frequency component of faces might be primarily processed already at the subcortical level (58). We, on the other hand, performed our extracellular recordings in the NCL, which is a higher-order processing area of the avian pallium (25). Hence, we might expect that the differences between LF and HF stimuli would be more pronounced at the earlier subcortical stages of processing (28, 59, 60).

The hypothesis that the detection of faces might occur already subcortically has not been directly tested at the level of single-cell responses in face-naïve newborn animals. However, responses to schematic face-like stimuli have been found in the superior colliculus of adult monkeys (59, 60). Our analyses of the SVM performance also offer indirect evidence that holistic detection of faces may occur in the subcortex. First of all, in the time-resolved analysis, the classifier successfully decoded the upright face stimulus shortly after the stimulus onset, which suggests the rapid detection of the face by the visual system. Second, in the categorization test, the upright face configuration did not overlap with responses to single facial elements. If the face-selective response would require separate detection and integration of single facial features (eyes and a beak), one could expect these stimuli to elicit a neural response similar to the upright face stimulus in the population of face-selective neurons. This was not the case, which indicates holistic processing of the face-like configuration. However, direct evidence for an innate subcortical face-processing mechanism can be provided only by neural recordings from subcortical areas in face-naïve young animals.

In addition to face-selective responses, our study revealed a considerable number of neurons responding to stimuli of different types. The number of selective responses to linear and inverted configurations was just above the chance level (P = 0.04), so it might be premature to make any assumptions about their potential biological function. However, a larger percentage of all recorded neurons (7%) showed a strong selectivity for the beak. The fact that these neurons did not respond to other one-element stimuli (left eye and right eye) suggests that their neural response was primarily triggered by the distinct position of the beak within the head silhouette. For birds, the beak is an important facial feature that provides a variety of signals, e.g., during feeding behavior [gulls (61)] or sexual displays [pigeons (3)]. Also in fowls, tidbitting serves as a salient cue for the presence of food, as a part of a mating display in adults and of a parental display performed by brooding hens (62, 63). Whether the observed beak-selective neural responses might be related to an innate component of these behaviors in domestic chickens remains to be established.

In summary, our study represents a significant step in revealing the innate neural mechanism of face detection. Neurons in the NCL of domestic chicks entirely devoid of any early-life experience with faces showed a strong selective response to the face-like stimuli. This means that the face detectors we observed in the chicks' brains are innate and do not require any prior experience.

Materials and Methods

Subjects. For the study six domestic chicks (*Gallus gallus domesticus*) from the Aviagen ROSS 308 strain were used. Fertilized eggs from a local commercial hatchery (CRESCENTI Società Agricola S.r.l.–AllevamentoTrepola–cod. Allevamento 127BS105/2) were incubated and hatched within incubators (Marans P140TU-P210TU) at 37.7 °C and 60% humidity in a dark room. After hatching in dark incubators, chicks were isolated and housed individually in metal cages (28 cm wide × 32 cm high × 40 cm deep) with nonreflective walls and floor covered with paper towels to prevent chicks from seeing their own reflection (Fig. 1 *C*, 2 and 3). Additionally, to exclude any occasional exposure to faces, the housing cages were placed on the upper shelf of the room, and all caretakers were wearing the black-painted face mask while feeding the chicks (Fig. 1 *C*, 1). Food and water were provided ad libitum, and animals were kept at a constant room temperature of 30 to 32 °C and a constant light–dark regime of 14 h light and 10 h dark. All experimental protocols were approved by the research ethics committee of the University of Trento and by the Italian Ministry of Health (permit number 539/2023-PR).

Experimental Setup. Experiments were performed in a rectangular-shaped arena (34 × 54 × 27 cm; W × L × H) with wooden walls and floor covered with nonreflective materials. One wall of the arena was replaced by a computer screen (AOC AGON AG271QG4, 144 Hz) used for stimuli presentation (Fig. 1*A*). The arena was divided in two sections by a metal grid placed 31 cm from the screen preventing chicks from directly approaching it and excluding reflections of the animal's face. To prevent chicks from seeing any faces, all habituation and experimental procedures including initial stages of the surgery until the animals were fully anesthetized were performed while wearing a full-face mask painted black (Fig. 1 *C*, 1). A custom-build automatic reward system consisted of a feeder with mealworms, whose lid was attached to a servo motor and controlled by Arduino Uno (Fig. 1*A*). Stimulus presentation and reward was controlled by Bonsai software with BonVision toolbox (64, 65).

Habituation Procedure. On the 2nd day post hatching, chicks learned to peck on mealworms. Between the 3rd and the 6th day after hatching the chicks were habituated to the setup. First, chicks were habituated to an empty head region (Fig. 1 *D*, 1) appearing on the screen. Initially, the birds received mealworms (the lid of the feeder opened for 500 to 1,000 ms) every time a stimulus appeared on the screen, which motivated them to pay attention to any new image appearing on the screen. During subsequent habituation, we gradually decreased the reward probability down to 30 to 40%, so that birds would still pay attention to the screen even without getting a mealworm. This procedure allowed us to minimize rewarding during actual recording sessions.

Surgery and Recordings. On the 7th day after hatching chicks were fully anesthetized using Isoflurane inhalation (1.5 to 2.0% gas volume, Vetflurane, 1,000 mg/g, Virbac, Italy) and placed in the stereotaxic apparatus with a bar fixed at the beaks' base and tilted 45° to ear bars. Local anesthesia (Emla cream, 2.5% lidocaine + 2.5% prilocaine, AstraZeneka, S.p.A.) was applied to the ears and skull skin before and after the surgery. Metal screws were placed into the skull for grounding and stabilization of the implant. A small craniotomy was made in the skull above the NCL (1.0 mm anterior to the bregma, 4.5 mm lateral to the midline, Fig. 2*A*) on the right hemisphere (five chicks) or on the left hemisphere (one chick). For extracellular recordings, we used self-wired tetrodes made out of formvar-insulated Nichrome wires (17.78 μm diameter, A-M Systems), which were gold-plated to reduce the impedance to 250 to 350 kOm (controlled by nanoZ, Plexon Inc.). Then, a commercially available Halo-5 microdrive (Neuralynx) was assembled according to the producer instructions, where four single tetrodes were put into polymicro tubes (inner diameter 0.1 mm) and glued to the plastic shuttles. The microdrive was implanted and fixed first with quick adhesive silicone (Kwik-Sil, World Precision Instruments) and then with dental cement (Henry Schein Krugg Srl, Italy).

After the surgery, the chicks were left to recover until the next day in their home cages. Between the 8th and the 12th day after hatching, we recorded neural responses to face-like stimuli in the NCL of chicks. Before every recording session, the microdrive was connected to the Plexon system (Plexon Inc.) via a QuickClip connector and an omnetics headstage (Neuralynx). After every recording session, the tetrodes were manually advanced by ca. 100 μm.

Signals were preamplified with a 16-channel head-stage (20×, Plexon Model number: PX.HST/16 V-G20-LN) subsequently amplified 1,000× and digitalized. Spike detection and sorting was automatically performed in Kilosort 2.0 (66) with following parameters: ops.minfr_goodchannels = 0.1; ops.Th = [10 5]; ops.lam = 20; ops.AUCsplit = 0.95; ops.ThPre = 8; ops.spkTh = −6. All identified units were manually curated using Phy 2.0.

Stimuli. To identify face-selective neural responses we used modified stimuli from previous behavioral experiments (4, 5) that showed innate preference of newborn chicks to face-like configurations (Fig. 1*D*). An empty head silhouette [13 × 9 cm (H × W), 23.7° × 16.5° visual angle, Fig. 1 *D*, 1] was used for habituation and as a background image during recordings. Therefore, in every trial only the configuration of dots (1.1 cm, 2° visual angle) inside this head region (Fig. 1 *D*, 2–10) or a range of frequency components (Fig. 1 *D*, 11 and 12) of the stimulus was changed. We defined a proper face detector based on its stronger neural response to the face-like configuration (Fig. 1 *D*, 2) than to other stimuli with three dots (an inverted face and a linear configuration; Fig. 1 *D*, 3 and 4) or to single facial features (eyes, a right eye, a left eye, and a beak; Fig. 1 *D*, 5–8).

In addition, we tested how face neurons responded to asymmetrical Picasso-like images (Fig. 1 *D*, 9 and 10) with eyes shifted to the left/right to the medial sagittal line of the upright face-like stimulus. We also tested the response of potential face neurons to face-like stimuli dominated by high-frequency (≥15 Hz, Fig. 1 *D*, 12) or low-frequency (≤5 Hz, Fig. 1 *D*, 11) components, which corresponds to ≥15.05 cycles/face (≥0.9 cycles/degree) and ≤4.95 cycles/face (≤0.3 cycles/degree), respectively. To modify the frequency components of the face-like stimulus we used the "hard_filter" function in Matlab applied to the original upright face-like image of 1,536 × 1,063 pixels. The filter was applied separately to three color channels, which were subsequently concatenated again.

During recording sessions, we randomly presented stimuli for 500 ms with interstimulus intervals randomly varying between 2,500 and 3,500 ms. Experiments were video-recorded using CineLAB system (Plexon Inc.). To enhance the motivation of birds to pay attention to the screen, random trials were occasionally randomly rewarded by opening the feeder 500 ms after the stimulus offset for 500 to 1,000 ms.

Histological Analysis. After the last neural recording birds were overdosed with the ketamine/xylazine solution (1:1 ketamine 10 mg/mL + xylazine 2 mg/mL). Electrolytic lesions were made at the recording sites by applying a high-voltage current to the tetrodes for 10 to 15 s. Then, the birds were perfused intracardially with the phosphate buffer (PBS; 0.1 mol, pH = 7.4, 0.9% sodium chloride, 5 °C) followed by 4% paraformaldehyde (PFA). Brains were incubated for at least two days in PFA and a further 2 d in 30% sucrose solution in PFA. Coronal 60 μm brain sections were cut at −20 °C using a cryostat (Leica CM1850 UV), mounted on glass slides, stained with the Giemsa dye (MG500, Sigma-Aldrich, St. Louis), and cover slipped with Eukitt (FLUKA). Brain sections were examined under the stereomicroscope (Stemi 508, Carl Zeiss, Oberkochen, Germany) to estimate the anatomical position of recording sites.

Data Analysis. Based on the visual analysis of video recordings, we selected only trials in which birds looked at the stimulus with both eyes or with the eye contralateral to the recording site. For the final analysis, we considered only those units from which we recorded at least 10 trials for each stimulus type (mean ± SD = 32 ± 7 trials per stimulus type). The rewarded trials were also included in the analysis, since the reward was provided randomly and equally often to all stimulus types: For every stimulus type, between 28% and 31% of all included trials were rewarded, with the upright stimulus being rewarded in 29% of trials. Therefore, the presence or expectation of a reward could not systematically affect the responses to any of the stimulus types over the others. Moreover, to exclude that the neural responses of face-selective neurons could differ between rewarded and unrewarded trials, we calculated the average firing rate within the face-selective window in response to the upright stimulus separately for rewarded and unrewarded trials. The paired t-test did not reveal any difference in the firing rate between rewarded and unrewarded trials ($t = -0.98$, $P = 0.34$), which confirms that the neural response to the upright stimulus was not affected by the presence of the reward.

Identification of face-selective neural responses. The neural activity of recorded units was analyzed in the 900 ms window starting from 100 ms after the stimulus onset [to account for the visual latency of NCL neurons (67)] until 500 ms after the stimulus offset. First, every trial was smoothed using Gaussian kernel with 100 ms sigma. To identify stimulus-selective neural responses we then performed a sliding-window ANOVA (one-way ANOVA; 10 ms bin window, 10 ms step-size) with the stimulus type as a factor (upright, inverted, linear, eyes, left eye, right eye, beak). For all significant ($P < 0.01$) time bins we performed a post hoc analysis ("multcompare" function with Tukey–Kramer test) and selected only bins where the response to the tested stimulus was significantly different ($P < 0.01$) from other stimuli. If we observed a significant response for at least a 100 ms period (10 consecutive bins) we performed an additional cluster permutation test to control for multiple comparisons. For this, all F-values within a significant response window were summed up (F-real) and compared to the sum of F-values resulting from the ANOVA and the post hoc analysis of randomly shuffled trials (F-shuffled). This procedure was repeated 1,000 times for every unit, and the response window was considered truly significant (i.e., face-selective) only if the F-real was higher than 95% of all F-shuffled (corresponding to a $P < 0.05$).

To estimate the probability of encountering false-positive responses in our dataset, we randomly sampled 224 trials (32 trials per 7 stimuli) out of all recorded trials (N = 119,567) for 1,000 times and, identical to real neurons, performed a sliding-window ANOVA with the post hoc test and the permutation test for each shuffled dataset to select false-positive units. We then compared the proportion of false-positive and real stimulus-selective units with the proportion test. Additionally, we compared the distribution of *p*-values of the selective windows obtained by the permutation test between real and false-positive units by performing a one-way ANOVA with stimulus type as a factor, followed by a post hoc comparison between pairs of stimuli (Tukey–Kramer test).

Analysis of response properties of face-selective cells. To quantify the selectivity of individual face-responsive cells we calculated a FSI (38), computed as the difference between the mean response to the face-like stimulus and the mean response to nonface stimuli, divided by the sum of these means. The mean response was defined as the average firing rate within the face-selective response window. FSI ≥ 0.33 or ≤−0.33 corresponds to a 2:1 ratio and are considered to signify a strong face-to-nonface neural response.

We tested the sensitivity of the face-selective neurons to violations of the symmetry of the face configuration. For this, we compared the firing rate within the face-selective window between the upright face-like configuration and Picasso-like stimuli. We expected face-selective cells with inhibitory response (with negative FSI) to show less inhibition in response to Picasso-like stimuli, and excitatory cells (with positive FSI) to decrease their response to Picasso-like stimuli. Therefore, we used a linear mixed effect model (LME) with stimulus type (upright, picassoL, picassoR) and FSI ("negative" or "positive") as fixed effects and "unitID" (43 face-selective units) as a random effect. For the post hoc analysis, we used the general linear hypothesis test ("glht" function from the "multcomp" package in R).

To investigate the response of face-selective units to different frequency components of the upright face-like stimulus, we compared the average firing rate within the face-selective response window between the high-frequency and the low-frequency stimuli. We did not perform a direct comparison between the frequency-modified images and the upright stimulus, since luminosity and contrast between these stimuli differed substantially and, thus, could be a confounding variable affecting the result. Therefore, we used the LME with stimulus type (HF, LF) and FSI (negative or positive) as fixed effects and unitID as a random effect. Pairwise comparisons were performed post hoc using the general linear hypothesis test.

Decoding of neural population responses. To quantify the amount of information about the face-like stimuli contained in the population response during the trial, we performed the PEV analysis. PEV measures the percentage (ω^2) of the variance explained by the tested factor. ω^2 is calculated from the sum of squares of the effect (*SSeffect*) and the mean squares of the within-group (error) variance (*MSerror*) (Eq. **1**).

$$\omega^2 = \frac{SSeffect - df * MSerror}{SStotal + MSerror}. \quad [\mathbf{1}]$$

Based on coefficients from the sliding-window ANOVA performed for each stimulus-responsive unit we calculated ω^2 for each 10 ms bin of the analyzed time window. To illustrate the explained variance for the entire population of units selective for a specific stimulus type, ω^2 values were averaged and compared to the average ω^2 obtained from the shuffled data (1,000 times for each unit). We identified the populations' information content to be significant when the ω^2 of real data was above the 95th percentile of the ω^2 from shuffled data (corresponding to $P < 0.05$).

To further evaluate how the neural population encodes face-like stimuli, we trained a multiclass SVM classifier to discriminate between face-like and nonface stimuli based on the neural response of face-selective NCL neurons. In this analysis, we included face-selective neurons that had at least 25 recorded trials per stimulus (N = 33 neurons). Every trial was smoothed using a Gaussian kernel with 100 ms sigma. Then, we randomly selected 25 trials per stimulus type and divided them into the training set (23 trials per stimulus type) and the test set (2 trials per stimulus type). To make the neural activity comparable between units, this was subsequently z-scored using the mean and the SD of the training set only. For a more robust estimation of the decoding accuracy, we performed one thousand iterations of the SVM training and testing, randomly selecting the trials each time. We trained the multiclass linear SVM in Matlab with the following parameters: "one-vs-one" classification, 10-fold cross-validation, linear kernel function, "auto" kernel scale, with no additional regularization. In the categorization test, we estimated the accuracy of the SVMs in categorization of face-like stimuli, including also the Picasso-like, the HF, and

the LF images (the responses to which had not been used for the initial selection of face-selective units).

In the generalization test, we trained SVMs to perform a binary face vs. non-face classification excluding one of the stimulus types from the training set. Subsequently, we tested the performance of the SVMs on the stimulus type not included into the training, to see whether these novel stimuli would be spontaneously classified as faces or nonfaces.

For both the categorization and the generalization test, we trained the SVMs on the average neural responses during the face-selective window for each unit. For the network trained on the face-selective window (categorization and generalization tests) the accuracy of the SVM predictions has been evaluated by the proportion test ($P < 0.05$).

Moreover, we aimed to estimate how the decoding accuracy changes during the stimulus presentation. For this analysis we performed the training and testing of the SVM for the whole duration of the trial smoothed by the Gaussian kernel (100 ms sigma) and divided into 10 ms bins, starting from 500 ms before the stimulus onset till 500 ms after the stimulus offset (overall duration 1,500 ms). To estimate the chance level and assess the significance of our SVM classifier's performance in the time-resolved categorization, we calculated the average accuracy across all stimulus categories during the 500 ms prestimulus interval. This period is assumed to reflect the natural variability of the data, serving as a baseline for chance-level performance. By combining data from 11 stimulus types over 50 time points (550 data points in total), we computed an average accuracy of 0.0816, consistent with chance accuracy (100/11 = 9%). To quantify the variability of this estimate, we calculated a 95% CI using the formula CI = norminv(1 − 0.05/2)*sqrt((0.0816* (1 − 0.0816))/550), resulting in a CI of 0.0816 ± 0.0229. This interval provides a threshold for evaluating the chance level, allowing us to determine whether the SVM's accuracy during the stimulus period is significantly above this baseline. We applied the same CI to the accuracy of the upright stimulus condition, considering the variability during prestimulus as reflecting the natural variability of the data.

All statistical analyses and visualization of the data was performed in R (68) with packages "tidyverse," multcomp, "ggplot2," and "PMCMRplus" and in MATLAB using custom-made scripts. The raw data and analyses scripts are available in the repository (69).

Data, Materials, and Software Availability. All data and code (Neural recordings and analysis script) for analyses are available in the main text or in the depository (10.5281/zenodo.10517792) (69).

ACKNOWLEDGMENTS. We would like to thank Uwe Mayer for his comments on the experimental design. We are also grateful to Anastasia Morandi-Raikova, to the people at the Animal House Facility for their help with handling the chicks, and Paul Hochstein for customizing nontransparent face-masks. This study has been supported by funding from the European Research Council under the European Union's Horizon 2020 research and Innovation Program No. 833504 SPANUMBRA (G.V.), PRIN 2017 ERC-SH4–A 2017PSRHPZ (G.V.), and PRIN 2022 PNRR–Grant Agreement P2022TKY7B (G.V.).

1. D. A. Leopold, G. A. Rhodes, Comparative view of face perception. *J. Comp. Psychol.* **124**, 233 (2010).
2. Y. Sugita, Face perception in monkeys reared with no exposure to faces. *Proc. Natl. Acad. Sci. U.S.A.* **105**, 394–398 (2008).
3. T. B. Patton, G. Szafranski, T. Shimizu, Male pigeons react differentially to altered facial features of female pigeons. *Behaviour* **147**, 757–773 (2010).
4. O. Rosa-Salva, L. Regolin, G. Vallortigara, Faces are special for newly hatched chicks: Evidence for inborn domain-specific mechanisms underlying spontaneous preferences for face-like stimuli. *Dev. Sci.* **13**, 565–577 (2010).
5. O. Rosa Salva, T. Farroni, L. Regolin, G. Vallortigara, M. H. Johnson, The evolution of social orienting: Evidence from chicks (*Gallus gallus*) and human newborns. *PLoS ONE* **6**, e18802 (2011).
6. M. Y. Wang, H. Takeuchi, Individual recognition and the 'face inversion effect' in medaka fish (*Oryzias latipes*). *elife* **6**, e24728 (2017).
7. M. J. Sheehan, E. A. Tibbetts, Specialized face learning is associated with individual recognition in paper wasps. *Science* **334**, 1272–1275 (2011).
8. S. D. Brown, R. J. Dooling, Perception of conspecific faces by budgerigars (*Melopsittacus undulatus*): I. Natural faces. *J. Comp. Psychol.* **106**, 203 (1992).
9. S. Watanabe, Y. Ito, Discrimination of individuals in pigeons. *Bird Behav.* **9**, 20–29 (1990).
10. J. Beránková, P. Veselý, J. Sýkorová, R. Fuchs, The role of key features in predator recognition by untrained birds. *Anim. Cogn.* **17**, 963–971 (2014).
11. C. Bruce, R. Desimone, C. G. Gross, Visual properties of neurons in a polysensory area in superior temporal sulcus of the macaque. *J. Neurophysiol.* **46**, 369–384 (1981).
12. D. I. Perrett, E. T. Rolls, W. Caan, Visual neurones responsive to faces in the monkey temporal cortex. *Exp. Brain Res.* **47**, 329–342 (1982).
13. N. Kanwisher, G. Yovel, The fusiform face area: A cortical region specialized for the perception of faces. *Philos. Trans. R. Soc. Lond. B, Biol. Sci.* **361**, 2109–2128 (2006).
14. K. Vinken, J. S. Prince, T. Konkle, M. S. Livingstone, The neural code for "face cells" is not face-specific. *Sci. Adv.* **9**, eadg1736 (2023).
15. M. H. Johnson, S. Dziurawiec, H. Ellis, J. Morton, Newborns' preferential tracking of face-like stimuli and its subsequent decline. *Cognition* **40**, 1–19 (1991).
16. E. Valenza, F. Simion, V. M. Cassia, C. Umiltà, Face preference at birth. *J. Exp. Psychol.: Hum. Percept. Perform.* **22**, 892 (1996).
17. V. M. Reid *et al.*, The human fetus preferentially engages with face-like visual stimuli. *Curr. Biol.* **27**, 1825–1828 (2017).
18. M. Buiatti *et al.*, Cortical route for facelike pattern processing in human newborns. *Proc. Natl. Acad. Sci. U.S.A.* **116**, 4625–4630 (2019).
19. H. L. Kosakowski *et al.*, Selective responses to faces, scenes, and bodies in the ventral visual pathway of infants. *Curr. Biol.* **32**, 265–274 (2022).
20. M. S. Livingstone *et al.*, Development of the macaque face-patch system. *Nat. Commun.* **8**, 14897 (2017).
21. M. J. Arcaro, P. F. Schade, J. L. Vincent, C. R. Ponce, M. S. Livingstone, Seeing faces is necessary for face-domain formation. *Nat. Neurosci.* **20**, 1404–1412 (2017).
22. S. Benetti *et al.*, Functional selectivity for face processing in the temporal voice area of early deaf individuals. *Proc. Natl. Acad. Sci. U.S.A.* **114**, E6437–E6446 (2017).
23. H. R. Rodman, S. P. Scalaidhe, C. G. Gross, Response properties of neurons in temporal cortical visual areas of infant monkeys. *J. Neurophysiol.* **70**, 1115–1136 (1993).
24. B. Duchaine *et al.*, The development of upright face perception depends on evolved orientation-specific mechanisms and experience. *iScience* **26**, 10 (2023).
25. O. Güntürkün, T. Bugnyar, Cognition without cortex. *Trends Cogn. Sci.* **20**, 291–303 (2016).
26. D. Kobylkov, U. Mayer, M. Zanon, G. Vallortigara, Number neurons in the nidopallium of young domestic chicks. *Proc. Natl. Acad. Sci. U.S.A.* **119**, e2201039119 (2022).
27. D. R. Wylie, C. Gutierrez-Ibanez, J. M. P. Pakan, A. N. Iwaniuk, The optic tectum of birds: Mapping our way to understanding visual processing. *Can. J. Exp. Psychol.* **63**, 328–338 (2009).
28. M. H. Johnson, Subcortical face processing. *Nat. Rev. Neurosci.* **6**, 766–774 (2005).
29. S. Watanabe, U. Mayer, H.-J. Bischof, Visual Wulst analyses "where" and entopallium analyses "what" in the zebra finch visual system. *Behav. Brain Res.* **222**, 51–56 (2011).
30. R. Pusch, W. Clark, J. Rose, O. Güntürkün, Visual categories and concepts in the avian brain. *Anim. Cogn.* **26**, 153–173 (2023).
31. Y. Bi, X. Wang, A. Caramazza, Object domain and modality in the ventral visual pathway. *Trends Cogn. Sci.* **20**, 282–290 (2016).
32. B. Duchaine, G. Yovel, A revised neural framework for face processing. *Annu. Rev. Vis. Sci.* **1**, 393–416 (2015).
33. N. Tinbergen, *The Herring Gull's World: A Study of The Social Behaviour of Birds* (Frederick A Praeger Inc., 1953).
34. D. Y. Tsao, M. S. Livingstone, Mechanisms of face perception. *Annu. Rev. Neurosci.* **31**, 411–437 (2008).
35. D. Kobylkov, G. Vallortigara, Face detection mechanisms: Nature vs. nurture. *Front. Neurosci.* **18**, 1404174 (2024).
36. T. Stein, M. V. Peelen, P. Sterzer, Adults' awareness of faces follows newborns' looking preferences. *PLoS ONE* **6**, e29361 (2011).
37. C. Turati, F. Simion, I. Milani, C. Umilta, Newborns' preference for faces: What is crucial? *Dev. Psychol.* **38**, 875 (2002).
38. D. Y. Tsao, W. A. Freiwald, R. B. Tootell, M. S. Livingstone, A cortical region consisting entirely of face-selective cells. *Science* **311**, 670–674 (2006).
39. K. M. Kendrick, B. A. Baldwin, Cells in temporal cortex of conscious sheep can respond preferentially to the sight of faces. *Science* **236**, 448–450 (1987).
40. T. Decramer *et al.*, Single-unit recordings reveal the selectivity of a human face area. *J. Neurosci.* **41**, 9340–9349 (2021).
41. S. Khuvis *et al.*, Face-selective units in human ventral temporal cortex reactivate during free recall. *J. Neurosci.* **41**, 3386–3399 (2021).
42. W. A. Freiwald, D. Y. Tsao, M. S. Livingstone, A face feature space in the macaque temporal lobe. *Nat. Neurosci.* **12**, 1187 (2009).
43. M. J. Arcaro, P. F. Schade, M. S. Livingstone, Universal mechanisms and the development of the face network: What you see is what you get. *Annu. Rev. Vis.* **5**, 341–372 (2019).
44. M. J. Arcaro, M. S. Livingstone, A hierarchical, retinotopic proto-organization of the primate visual system at birth. *eLife* **6**, e26196 (2017).
45. J. Rose, A. M. Schiffer, L. Dittrich, O. Güntürkün, The role of dopamine in maintenance and distractability of attention in the "prefrontal cortex" of pigeons. *Neuroscience* **167**, 232–237 (2010).
46. D. Lengersdorf, R. Pusch, O. Güntürkün, M. C. Stüttgen, Neurons in the pigeon nidopallium caudolaterale signal the selection and execution of perceptual decisions. *Eur. J. Neurosci.* **40**, 3316–3327 (2014).
47. D. Scarf, M. Stuart, M. Johnston, M. Colombo, Visual response properties of neurons in four areas of the avian pallium. *J. Comp. Physiol. A* **202**, 235–245 (2016).
48. W. J. Clark, B. Porter, M. Colombo, Searching for face-category representation in the avian visual forebrain. *Front. Physiol.* **10**, 140 (2019).
49. W. Clark *et al.*, Neurons in the pigeon visual network discriminate between faces, scrambled faces, and sine grating images. *Sci. Rep.* **12**, 589 (2022).
50. F. Simion, E. Valenza, V. Macchi Cassia, C. Turati, C. Umiltà, Newborns' preference for up–down asymmetrical configurations. *Dev. Sci.* **5**, 427–434 (2002).
51. G. Passalis, P. Perakis, T. Theoharis, I. A. Kakadiaris, Using facial symmetry to handle pose variations in real-world 3D face recognition. *IEEE PAMI* **33**, 1938–1951 (2011).

52. Y. Kowataria, S. Yamane, M. Yamamoto "Realistic and nonrealistic art works of human portrait activated different cortical neural networks" in *Neuronal Network Research Horizons* (Nova Biomedical, 2007), p. 227.
53. N. P. Costen, D. M. Parker, I. Craw, Effects of high-pass and low-pass spatial filtering on face identification. *Percept. Psychophys.* **58**, 602–612 (1996).
54. F. J. Hsiao, J. C. Hsieh, Y. Y. Lin, Y. Chang, The effects of face spatial frequencies on cortical processing revealed by magnetoencephalography. *Neurosci. Lett.* **380**, 54–59 (2005).
55. C. Jeantet, S. Caharel, R. Schwan, J. Lighezzolo-Alnot, V. Laprevote, Factors influencing spatial frequency extraction in faces: A review. *Neurosci. Biobehav. Rev.* **93**, 123–138 (2018).
56. E. T. Rolls, G. C. Baylis, C. M. Leonard, Role of low and high spatial frequencies in the face-selective responses of neurons in the cortex in the superior temporal sulcus in the monkey. *Vis. Res.* **25**, 1021–1035 (1985).
57. H. Halit, M. De Haan, P. G. Schyns, M. H. Johnson, Is high-spatial frequency information used in the early stages of face detection? *Brain Res.* **1117**, 154–161 (2006).
58. P. Vuilleumier, J. L. Armony, J. Driver, R. J. Dolan, Distinct spatial frequency sensitivities for processing faces and emotional expressions. *Nat. Neurosci.* **6**, 624–631 (2003).
59. M. N. Nguyen *et al.*, Neuronal responses to face-like and facial stimuli in the monkey superior colliculus. *Front. Behav. Neurosci.* **8**, 85 (2014).
60. Q. V. Le *et al.*, A prototypical template for rapid face detection is embedded in the monkey superior colliculus. *Front. Syst. Neurosci.* **14**, 5 (2020).
61. C. ten Cate *et al.*, Tinbergen revisited: A replication and extension of experiments on the beak colour preferences of herring gull chicks. *Anim. Behav.* **77**, 795–802 (2009).
62. C. L. Smith, C. S. Evans, Silent tidbitting in male fowl, *Gallus gallus*: A referential visual signal with multiple functions. *J. Exp. Biol.* **212**, 835–842 (2009).
63. A. W. Stokes, Parental and courtship feeding in red jungle fowl. *The Auk* **88**, 21–29 (1971).
64. G. Lopes *et al.*, Bonsai: An event-based framework for processing and controlling data streams. *Front. Neuroinf.* **9**, 7 (2015).
65. G. Lopes *et al.*, Creating and controlling visual environments using BonVision. *eLife* **10**, e65541 (2021).
66. M. Pachitariu, S. Sridhar, C. Stringer, Solving the spike sorting problem with Kilosort. bioRxiv [Preprint] (2023). https://doi.org/10.1101/2023.01.07.523036 (Accessed 3 September 2024).
67. L. Veit, K. Hartmann, A. Nieder, Neuronal correlates of visual working memory in the corvid endbrain. *J. Neurosci.* **34**, 7778–7786 (2014).
68. R Core Team, *R: A Language and Environment for Statistical Computing* (R Foundation for Statistical Computing, 2017). www.R-project.org/.
69. D. Kobylkov, O. Rosa-Salva, M. Zanon, G. Vallortigara, Innate face detectors in the endbrain of young domestic chicks. Zenodo. https://zenodo.org/records/10517793. Deposited 16 January 2024.